Pediatric Radiology (2020) 50:224–233
https://doi.org/10.1007/s00247-019-04537-8

ORIGINAL ARTICLE

Fetal magnetic resonance imaging of skeletal dysplasias

Leah A. Gilligan[1] · Maria A. Calvo-Garcia[1,2] · K. Nicole Weaver[3,4] · Beth M. Kline-Fath[1,2]

Received: 14 June 2019 / Revised: 19 August 2019 / Accepted: 16 September 2019 / Published online: 27 November 2019

Abstract

Background Fetal magnetic resonance imaging (MRI) is obtained for prenatal diagnosis and prognostication of skeletal dysplasias; however, related literature is limited.

Objective The purpose of this study was to define the utility of fetal MRI for skeletal dysplasias and to report MRI findings associated with specific diagnoses.

Materials and methods This retrospective study was approved by the institutional review board; informed consent was waived. Women referred for suspected fetal skeletal dysplasia who underwent MRI between January 2003 and December 2018 were included. Definitive diagnoses were determined by genetic testing, autopsy, physical examination and/or postnatal/postmortem imaging. Fetal MRI examinations and reports were reviewed. Descriptive statistics were used to summarize imaging findings.

Results Eighty-nine women were referred for fetal MRI for possible skeletal dysplasia. Forty-three (48%) were determined to have a diagnosis other than skeletal dysplasia and nine were excluded for lack of specific skeletal dysplasia diagnosis. Thirty-seven cases of skeletal dysplasia with available fetal MRI and specific diagnosis were included for analysis. Diagnoses included achondrogenesis (n=2), achondroplasia (n=5), Boomerang dysplasia (n=1), campomelic dysplasia (n=2), Jeune syndrome (n=1), Kniest dysplasia (n=1), osteogenesis imperfecta (n=15) and thanatophoric dysplasia (n=10). A specific skeletal dysplasia diagnosis was mentioned in 17/37 (46%) of MRI imaging reports and correct for 14/17 (82%). MRI findings were reported for each specific skeletal dysplasia diagnosis.

Conclusion Fetal MRI is a useful diagnostic tool for skeletal dyplasias and excluded the diagnosis in nearly half of referred pregnancies. In addition to providing fetal lung volumes, fetal MRI demonstrates findings of the brain in achondroplasia and thanatophoric dysplasia, of the spine in achondroplasia and achondrogenesis, of the calvarium in osteogenesis imperfecta and thanatophoric dysplasia, and of the cartilage in Kniest dysplasia.

Keywords Achondroplasia · Fetus · Magnetic resonance imaging · Osteogenesis imperfecta · Skeletal dysplasia · Thanatophoric dysplasia

Introduction

Skeletal dysplasias are a large, heterogeneous group of osteochondrodysplasias, or disorders of the skeleton. Skeletal dysplasias manifest with one or more bone findings including abnormal length, shape, number and/or density. They encompass more than 400 specific diagnoses, for which associated mutations in more than 300 genes have been identified and for which phenotypes and outcomes vary, respectively, from mild and good to severe and lethal [1]. Grouped together, skeletal dysplasias occur at a rate of 1 in 3,000 to 5,000 live births [2]. Severe skeletal dysplasias are often detected by routine prenatal ultrasound (US) examination around 20 weeks' gestation. Furthermore, antenatal sonography is highly accurate for predicting the lethality of skeletal

✉ Leah A. Gilligan
leah.gilligan@mchs.com

[1] Department of Radiology, Cincinnati Children's Hospital Medical Center, 3333 Burnet Ave., MLC 5031, Cincinnati, OH 45229, USA

[2] Department of Radiology, University of Cincinnati College of Medicine, Cincinnati, OH, USA

[3] Division of Human Genetics, Cincinnati Children's Hospital Medical Center, Cincinnati, OH, USA

[4] Department of Pediatrics, University of Cincinnati College of Medicine, Cincinnati, OH, USA

dysplasias, usually related to the degree of pulmonary hypoplasia that can be estimated on US with biometric ratios [3–8]. Additionally, US allows an accurate assessment of the severity and distribution of long bone shortening, degree of bone mineralization, and presence of bowing deformities, fractures, polydactyly or other features of the hands, calvarium and face.

However, prenatal US for skeletal dysplasia diagnosis has limitations because of the low incidence, many possible specific diagnoses, overlapping features and phenotypic variability of skeletal dysplasias. Furthermore, some skeletal dysplasias may not be detected until the late third trimester and technical factors such as large maternal body habitus and oligohydramnios may affect fetal detail [9]. Some studies have reported about 40–60% accuracy of prenatal US for establishing a specific skeletal dysplasia diagnosis, while one series reported an overall accuracy of 68% that increased to 88–89% for detecting lethal skeletal dysplasias (thanatophoric dysplasia and osteogenesis imperfecta) [4, 6, 10, 11]. In most clinical settings, subsequent prenatal imaging may be performed for further work-up of a suspected skeletal dysplasia with uncertain diagnosis and/or prognosis to provide additional information for clinical decision making (whether to perform amniocentesis, direction for specific genetic testing, delivery planning, etc.). However, practices patterns vary. For example, at some institutions, low-dose fetal computed tomography (CT) has been shown to have superior diagnostic accuracy compared to US [12, 13]. At our institution, fetal magnetic resonance imaging (MRI) is obtained for further prenatal work-up of skeletal dysplasia. Furthermore, fetal MRI accurately assesses lung volume, which is strongly correlated with lethality in the setting of skeletal dysplasia [14]. However, while several case reports of skeletal dysplasias with fetal MRI have been reported, there is a lack of published studies evaluating the utility of fetal MRI for prenatal diagnosis and prognostication beyond fetal lung volume data [14–20].

The purpose of this study was to define the utility of fetal MRI for skeletal dysplasia. We also aimed to identify findings on MRI associated with specific skeletal dysplasia diagnoses and measure their diagnostic accuracies. We hypothesized that fetal MRI would complement prenatal US for the diagnosis and prognostication of skeletal dysplasia and that it would be especially helpful in identifying brain, spine or cartilage abnormalities.

Materials and methods

An institutional review board approved this retrospective, single-center, Health Insurance Portability and Accountability Act (HIPAA)-compliant study. A waiver of informed consent was granted.

All women who had a fetus with suspected skeletal dysplasia or a limb abnormality detected on prenatal US and were referred to our institution for additional imaging and/or genetic consultation and who underwent at least one fetal MRI during their pregnancy between January 2003 and December 2018 were eligible for inclusion in this study. Pregnancies with skeletal dysplasia were identified via a query of software held in the Department of Radiology (Insight; Softek Illuminate, Overland Park, KS) and a database from the Cincinnati Fetal Care Center.

Our institutional electronic medical record (Epic; Epic Systems Corp., Verona, WI) and radiology picture archiving and communication system (Merge; IBM Watson, Chicago, IL) were reviewed to derive imaging, genetics, pathology and pregnancy outcome data. This included a review of the radiology reports of fetal MRI examinations from which the indication for examination, maternal and gestational age, imaging findings and suggested diagnoses were recorded. We also reviewed the results of any genetic testing for skeletal dysplasia (done pre- or postnatally), autopsy, and relevant postnatal or postmortem imaging, including skeletal survey and MRI necropsy.

We considered the results of genetic testing to be the diagnostic gold standard for specific skeletal dysplasia diagnosis. However, for fetuses/infants without an identified genetic mutation, the definitive diagnosis was defined via data from autopsy, postnatal/postmortem physical examination and/or postnatal/postmortem imaging. In fetuses/infants without a definitive diagnosis of a specific skeletal dysplasia, but in whom a specific skeletal dysplasia diagnosis was presumed via data from prenatal imaging, including characteristic US and MRI features, the presumed, specific skeletal dysplasia diagnosis was used for our analysis (for thanatophoric dysplasia or osteogenesis imperfect only). Fetuses were excluded if assigned a nonskeletal dysplasia diagnosis or if a specific skeletal dysplasia diagnosis was never assigned.

Fetal MRI protocol

All fetal MRI examinations were performed on a 1.5-Tesla magnet using a Philips (Philips Healthcare, Andover, MA) or GE (General Electric Healthcare, Waukesha, WI) system. The skeletal dysplasia imaging protocol included axial, sagittal and coronal T2-weighted half-acquisition single-shot fast spin echo (SSFSE) and true fast imaging with steady-state precession (FISP)/fast imaging employing steady-state acquisition (FIESTA) images of the thorax, abdomen at 4 mm (no skip) slice thickness. SSFSE T2-weighted imaging through the brain was performed at a slice thickness of 3 mm (no gap) below 24 weeks and 4 mm (no gap) after 24 weeks. Imaging after 2016 also included echo-planar images of the fetal skeleton at 5-mm slice thickness without a skip in the sagittal and coronal planes. The smallest fields of view

possible were utilized. However, given the retrospective nature and wide timeline of cases included in this study, the imaging protocol was not standardized across all cases. Additionally, outside fetal MRI examinations uploaded to the electronic medical record and interpreted at our institution were also included in our study.

For clinical purposes, a radiologist created an imaging report for the fetal MRI following the examination and may have had relevant clinical information (genetics work-up, prenatal ultrasound images and/or report) available to her/him. As mentioned, these reports were retrospectively reviewed, and all findings were recorded. In patients with more than one fetal MRI, only the first examination was reviewed for imaging findings, as repeat fetal MRIs, when performed, were obtained for lung volume calculation. One pediatric radiologist with more than 15 years of experience in fetal imaging (B.M.K.-F.) retrospectively reviewed reports and images from the fetal MRI examinations to confirm previously reported findings and to establish additional findings.

Statistical analysis

Continuous data were summarized as means and standard deviations (SD); categorical data were summarized as counts and percentages. Patients with the same specific skeletal dysplasia diagnosis were grouped together for analysis. We also grouped cases into two cohorts based on year of MRI (early cases: 2004 to 2009; later cases: 2010 to 2018) given improved radiologist experience with fetal MRI for SD. Fisher exact test (two-tailed) was performed to compare frequencies. *P*-values <0.05 were considered statistically significant for inference testing. Analyses were performed using Microsoft Office Excel 2013 (Microsoft Corp., Redmond, WA).

Results

Eighty-nine women were eligible for inclusion in the study. Of these, 43 (48%) were excluded for having a diagnosis other than skeletal dysplasia. These patients had, instead, the following diagnoses suspected on MRI and/or genetics evaluation: arthrogryposis (*n*=4), caudal regression syndrome (*n*=3), chromosomal duplication syndromes (*n*=2), Cornelia de Lange syndrome (*n*=2), ectrodactyly syndrome (*n*=1), Holt-Oram syndrome (*n*=1), limb reduction anomalies (*n*=9), limb body wall complex (*n*=1), mandibulofacial dysostosis (*n*=1), Shwachman-Diamond syndrome (*n*=1), Treacher Collins (*n*=1), VACTERL (vertebral defects, anal atresia, cardiac defects, trachea-esophageal fistula, renal anomalies and limb abnormalities; *n*=3), Wolf-Hirschhorn disease (*n*=1) or an unknown diagnosis (*n*=13). Of the 46 fetuses (52%) determined to have a skeletal dysplasia, 9 (20%) were never assigned a specific skeletal dysplasia diagnosis and were excluded. These cases included pregnancies with unknown diagnosis due to fetal or neonatal demise within hours of birth (*n*=5), termination (*n*=1), lost to follow-up (*n*=2) and normal skeletal dysplasia panel but likely unidentified gene resulting in skeletal dysplasia (*n*=1). Of note, three of the excluded cases were consistent with skeletal dysplasia favored to represent either Ellis Van Crevald or Jeune syndrome, but confirmation of diagnosis was not achieved. The remaining 37 patients were included in this study. In this group, 26 (70%) fetal MRI examinations were performed at our institution; the remaining 11 examinations had been uploaded to our institutional PACS. On average, 2.5 cases were seen per year, and 18 (49%) examinations were performed after 2009.

Of the 37 patients included in our study, mean maternal age was 29±6 years (range: 18–43 years) and mean gestational age was 26±5 weeks (range: 18 weeks, 1 day–36 weeks, 5 days) at the time of MRI examination. All fetal MRI examinations were performed for the indication of skeletal dysplasia, and 7/37 (19%) of the MRI reports mentioned additional indications for examination, including other congenital anomalies, cystic hygroma and hydrocephalus. Four MRI reports documented a specific diagnosis as the indication for examination (all were osteogenesis imperfecta and one of these four cases was determined to be osteogenesis imperfecta with subsequent work-up) while the remainder of MRI reports included only skeletal dysplasia in the indication for examination.

Table 1 summarizes the specific skeletal dysplasia diagnoses, confirmatory genetic testing and other diagnostic data obtained for the 37 patients. Table 2 summarizes the fetal outcomes (living at 3 months of age], neonatal demise [death within 3 months of life], intrauterine fetal demise, termination, or unknown.), grouped per specific skeletal dysplasia diagnosis.

Diagnostic performance of fetal MRI for skeletal dysplasias

Table 3 summarizes the accuracy of specific skeletal dysplasia diagnoses mentioned in the radiology reports. A favored specific skeletal dysplasia diagnosis was only mentioned in the MRI report impression for 17 (46%) of the 37 cases. When a specific skeletal dysplasia diagnosis was offered by fetal MRI, the diagnosis was correct 82% (14/17) of the time, for an overall rate of correct, specific skeletal dysplasia diagnosis in our included cases of 38% (14/37). When divided into early and later MRI cohorts by year, there was a significantly higher frequency of cases for which a specific skeletal dysplasia diagnosis was reported in the later MRI cohort (72% [later period] vs. 21% [early period], *P*=0.0029). However, there was no statistical difference in the accuracy of the specific skeletal dysplasia diagnosis mentioned in the MRI report between the early (75%) and late (85%) cohorts (*P*=1.0).

Table 1 Skeletal dysplasia diagnosis data

Diagnosis	*n* (%)	Number with genetic testing performed (%)	Number with identified mutation (%) [gene]	Source of diagnosis for cases without identified gene mutation
Achondrogenesis[a]	2 (5)	0	0	Postmortem physical examination (*n*=1), MRI necropsy and autopsy (*n*=1)
Achondroplasia	5 (14)	4 (80)	4 (80) [FGFR3]	Postnatal skeletal survey (*n*=1)
Boomerang dysplasia	1 (3)	0	1 (100) [FNLA]	n/a
Campomelic dysplasia	2 (5)	2 (100)	0	Autopsy and postmortem skeletal survey (*n*=1), postnatal skeletal survey and physical examination (*n*=1)
Jeune syndrome	1 (3)	1 (100)	0	Autopsy and postmortem skeletal survey (*n*=1)
Kniest dysplasia	1 (3)	1 (100)	1 (100) [COL2A1]	n/a
Osteogenesis imperfecta (OI)	15 (41)	10 (67)	10 (67) [COL1A1 (*n*=8), COL1A2 (*n*=2)]	Autopsy and/or postmortem skeletal survey (*n*=3), postnatal physical exam (*n*=1), geneticist confirmed by prenatal imaging (*n*=1)
OI, Type II	7 (47)	3 (43)	3 (43) [COL1A1]	Autopsy and/or postmortem skeletal survey (*n*=3), geneticist confirmed by prenatal imaging (*n*=1)
OI, Type III[b]	7 (47)	6 (86)	6 (86) [COL1A1 (*n*=4), COL1A2 (*n*=2)]	Postnatal physical examination (*n*=1)
OI, Type IV	1 (7)	1 (100)	1 (100) [COL1A1]	n/a
Thanatophoric dysplasia	10 (27)	4 (40)	4 (40) [FGFR3]	Autopsy and postmortem skeletal survey (*n*=1), postnatal physical examination (*n*=3), geneticist confirmed by prenatal imaging (*n*=2)
Total	37	22 (59)	20 (54)	n/a

[a] Both cases were achondrogenesis Type II

[b] One case of OI Type III had a concomitant diagnosis of Stickler syndrome and had two identified mutations in COL1A2

COL1A1 collagen type 1 alpha 1 chain, *COL1A2* collegen type 1 alpha 2 chain, *COL2A1* collagen type 2 alpha 1 chain, *FGFR3* fibroblast growth factor receptor 3, *FNLA* filamin A, *n/a* not applicable

Findings of skeletal dysplasias on fetal MRI

The pertinent findings observed on fetal MRI for each specific skeletal dysplasia diagnosis are presented in Table 4. Of note, the findings of short limbs and narrow chest are not included in these tables as they are nonspecific and were observed in most included cases. Additionally, there were no specific findings observed in the case of Jeune syndrome, so this diagnosis is not included in Table 4. Representative cases for diagnostic findings associated with specific skeletal dysplasia diagnoses are demonstrated in Figs. 1-5.

Discussion

Given the wide spectrum of phenotypes, differences in outcomes and varied management strategies across the many types of skeletal dysplasias, a thorough prenatal work-up and multidisciplinary team approach to patient counseling is of great value. At our institution, care conferences for women with a fetus with skeletal dysplasia typically include members from maternal-fetal medicine, genetics, radiology, neonatology and, sometimes, surgery and/or cardiology, and take into account several sources of data, including patient history, imaging (prenatal US and, often, fetal MRI) and genetic testing. Anecdotally, fetal MRI has provided data valuable for diagnostication and prognostication of skeletal dysplasia at our center; however, there is a paucity of published literature regarding the utility of fetal MRI for skeletal dysplasia, perhaps related to the low prevalence of skeletal dysplasia and geographical differences in practice patterns. Thus, in this study, we retrospectively reviewed cases of skeletal dysplasia with fetal MRI to assess the diagnostic performance and typical findings of fetal MRI for skeletal dysplasia.

We have first demonstrated that many patients who were referred for fetal MRI for suspected skeletal dysplasia did not ultimately have a fetus with a skeletal dysplasia. In fact, this was true for almost half of the referred patients, which may be related to the methodology of our study (e.g., we generously searched for and initially included patients so as to not accidentally miss a case of skeletal dysplasia) but may also be explained by the multitude of syndromes that include limb anomalies but are not due to an underlying skeletal dysplasia, for example, VACTERL. However, in these cases, fetal MRI

Table 2 Skeletal dysplasia pregnancy outcome data

Diagnosis	Living[a] (%)	Neonatal demise[b] (%)	Intrauterine fetal demise (%)	Termination (%)	Unknown (%)
Achondrogenesis	0	0	2 (100)	0	0
Achondroplasia	5 (100)	0	0	0	0
Boomerang dysplasia	0	1 (100)	0	0	0
Campomelic dysplasia	1 (50)	1 (50)	0	0	0
Jeune syndrome	0	0	1 (100)	0	0
Kniest dysplasia	1 (100)	0	0	0	0
Osteogenesis imperfecta (OI)	8 (53)	3 (20)	2 (13)	2 (13)	0
OI, Type II	0	3 (43)	2 (29)	2 (29)	0
OI, Type III	7 (100)	0	0	0	0
OI, Type IV	1 (100)	0	0	0	0
Thanatophoric dysplasia	0	7 (70)	1 (10)	1 (10)	1 (10)[c]
Total	15 (41)	12 (32)	6 (16)	3 (8)	1 (3)

[a] Living at 3 months of age

[b] Death within 3 months of age

[c] Patient lost to follow-up, had positive genetic testing for thanatophoric dysplasia

was useful in that it either excluded a diagnosis of skeletal dysplasia or proposed one or more alternative(s), nonskeletal dysplasia diagnoses. Another interesting, but unsurprising, finding of our study was that about one-fifth of the cases of skeletal dysplasia never received an exact diagnosis. Again, this was predominantly due to intrauterine loss or demise within hours of birth without prenatal testing, termination, loss of postnatal follow-up, or negative genetics work-up. Importantly, these two cohorts were excluded from our study to allow us to make more impactful conclusions.

In the cohort of included patients who had a specific skeletal dysplasia diagnosis mentioned in the impression of the fetal MRI examination report, we found that the suggested diagnosis was accurate about 82% of the time. Additionally, we have demonstrated that in the first half of fetal MRI examinations, done from 2004 to 2009, radiologists less frequently reported an exact skeletal dysplasia diagnosis and instead offered a general diagnosis of skeletal dysplasia in the report impression, while in the latter half of examinations, done between 2010 and 2018, radiologists offered an exact skeletal dysplasia diagnosis for 72% of cases. We believe this is related

Table 3 Diagnostic performance of all fetal MRIs (2004 to 2018) for specific skeletal dysplasia diagnosis

Diagnosis	Favored diagnosis correct (%)	Favored diagnosis(es) incorrect (%)	No specific skeletal dysplasia diagnosis offered (%)
Achondrogenesis	2 (100)[a]	0	0
Achondroplasia	1 (20)	0	4 (80)
Boomerang dysplasia	0	0	1 (100)
Campomelic dysplasia	0	2 (100)[b]	0
Jeune syndrome	0	0	1 (100)
Kniest dysplasia	1 (100)[c]	0	0
Osteogenesis imperfecta (OI)	4 (27)	1 (7)	10 (67)
OI, Type II	3 (43)	0	4 (57)
OI, Type III	1 (14)	1 (14)[d]	5 (71)
OI, Type IV	0	0	1 (100)
Thanatophoric dysplasia	6 (60)	0	4 (40)
Total	14 (38)	3 (8)	20 (54)

[a] In one case, two favored diagnoses were offered: achondrogenesis and hypochondrogenesis

[b] In one case, osteogenesis imperfecta was favored. In the other case, a wide differential of non-skeletal dysplasia diagnoses were offered

[c] Three favored diagnoses were offered: Kniest dysplasia, spondoepiphyseal dysplasia and Stickler syndrome

[d] The diagnosis of short rib polydactyly syndrome was offered

Table 4 Summary of MRI findings in fetuses grouped per specific skeletal dysplasia diagnosis

Diagnosis	Mean gestational age at time of MRI (weeks)	MRI finding	Number of cases
Achondrogenesis (*n*=2)	26.7±3.5	**Skeletal findings**	
		Narrow vertebral bodies	2
		Poor spine mineralization	2
Achondroplasia (*n*=5)	34.6±1.9	**Brain findings**	
		Prominent extraaxial spaces	5
		Deep transverse sulcus	5
		Oversulcation of the temporal lobe	5
		Incomplete hippocampal rotation	4
		Spine findings	
		Thoracolumbar kyphosis	4
		Small spinal canal	4
		Narrow craniocervical junction	4
Boomerang dysplasia (*n*=1)	30.2	**Miscellaneous findings**	
		Omphalocele	1
Campomelic dysplasia (*n*=2)	22.0±2.0	**Skeletal findings**	
		Limb bowing	2
		Club feet	2
		Micrognathia	1
Kniest dysplasia (*n*=1)	26.4	**Skeletal findings**	
		Abnormal epiphyseal centers	1
		Prominent costal areas	1
		Enlarged disc spaces	1
Osteogenesis imperfecta (OI) (*n*=15)	24.1±6.9	**Skeletal findings**	
		Limb bowing	15
		Poorly ossified calvarium	7
OI, Type II (*n*=7)		**Skeletal findings**	
		Limb bowing	7
		Poorly ossified calvarium	5
OI, Type III (*n*=7)		**Skeletal findings**	
		Limb bowing	7
		Poorly ossified calvarium	2
OI, Type IV (*n*=1)		**Skeletal findings**	
		Limb bowing	1
Thanatophoric dysplasia (*n*=10)	23.8±3.4	**Brain findings**	
		Temporal lobe sulcation abnormality	10
		Skeletal findings	
		Abnormal calvarial contour	10
		Limb bowing	7

to the radiologists' improved experience with skeletal dysplasias on fetal MRI over time. From this data, we make two conclusions: Fetal MRI is a valuable tool for skeletal dysplasia diagnosis as a supplement to sonography, and pediatric radiologists who have experience in fetal MRI for skeletal dysplasia are more likely to provide an exact skeletal dysplasia diagnosis.

Notably, in this study, we did not compare the diagnostic accuracy of fetal MRI with that of prenatal US for skeletal dysplasia. However, previous studies have shown the accuracy of prenatal US for exact skeletal dysplasia diagnosis to be about 40–80%, which is lower to equivalent to what we demonstrated for fetal MRI in our study [4, 6, 10, 11]. Thus, fetal MRI could be a useful adjunct to prenatal US for skeletal dysplasia diagnosis. A similar conclusion was made by Berceanu et al. [17] in a case study that compared US and MRI findings for prenatal diagnosis of skeletal dysplasia, and, to our knowledge, there are no other similar published studies.

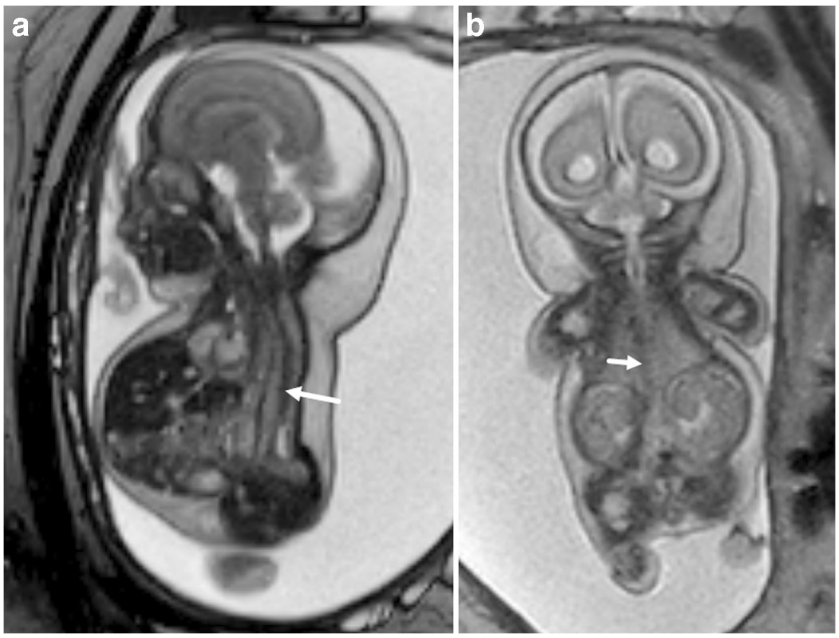

Fig. 1 Fetus with achondrogenesis at 26 weeks. **a** Sagittal steady-state free precession (SSFP) T2-weighted image demonstrates abnormal T2 hyperintense vertebrae (*arrow*) due to lack of ossification. **b** Coronal single-shot fast spin echo (SSFSE) T2-weighted image shows abnormal T2 hyperintense spine (*arrow*) but also small chest and limbs. The fetus had hydrops (soft-tissue edema and ascites)

Advantages of fetal MRI include lack of ionizing radiation and improved contrast and resolution, especially of the brain and soft tissues [21]. Therefore, it is unsurprising that literature that mentions MRI for skeletal dysplasia is in context of evaluation of the brain, spinal cord, spine, cartilage, and/or lung volumes or when US evaluation is limited by oligohydramnios [10, 14, 22, 23]. Many of the findings of skeletal dysplasia by fetal MRI observed in our study were, indeed, of the brain or spine. Furthermore, skeletal dysplasias with typical brain or spine findings (achondrogenesis, achondroplasia and thanatophoric dysplasia) comprised almost half of the cases in our study. Of note, our study did not explore the diagnostic utility of lung volumes by fetal MRI, as it has been previously demonstrated [14]. Altogether, these observations are convincing evidence to support the use of fetal MRI for skeletal dysplasia.

We found two findings unique to thanatophoric dysplasia in our study population: temporal lobe sulcation changes (deep and transverse temporal sulci) and abnormal calvarial contour (spectrum of cloverleaf skull), evidencing the strong diagnostic performance of fetal MRI for diagnosis of thanatophoric dysplasia. These findings have been reported on fetal MRI in a case study and on prenatal US in a previous case series [15, 24]. Temporal lobe abnormalities have been previously described in other fibroblast growth factor receptor (FGFR)-related conditions, such as achondroplasia, hypochondroplasia, and Apert and Pfeiffer syndromes, so the presence of any temporal lobe abnormality is not entirely specific; however, these other syndromes do not have the severity of limb shortening or narrow chest that is present in thanatophoric dysplasia [25]. Given the good diagnostic performance of fetal MRI for identifying thanatophoric dysplasia

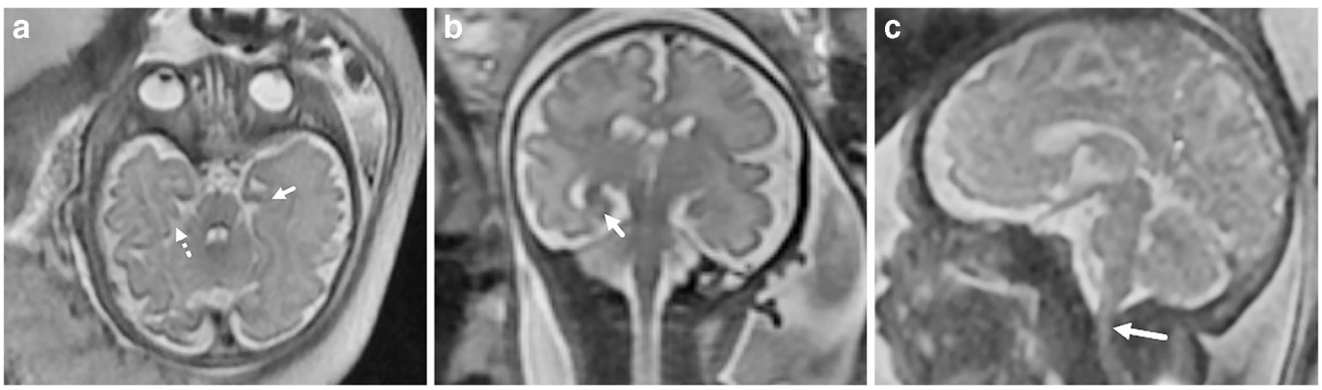

Fig. 2 Achondroplasia in a fetus at 33 weeks. **a** Axial single-shot fast spin echo (SSFSE) T2-weighted image of the brain shows the deep transverse sulcus in the temporal lobe (*solid arrow*) and oversulcation (*dotted arrow*). **b** Coronal SSFSE T2-weighted imaging demonstrates incomplete hippocampal rotation (*arrow*). **c** Sagittal SSFSE T2-weighted image of the brain in a fetus with narrow craniocervical junction (*arrow*)

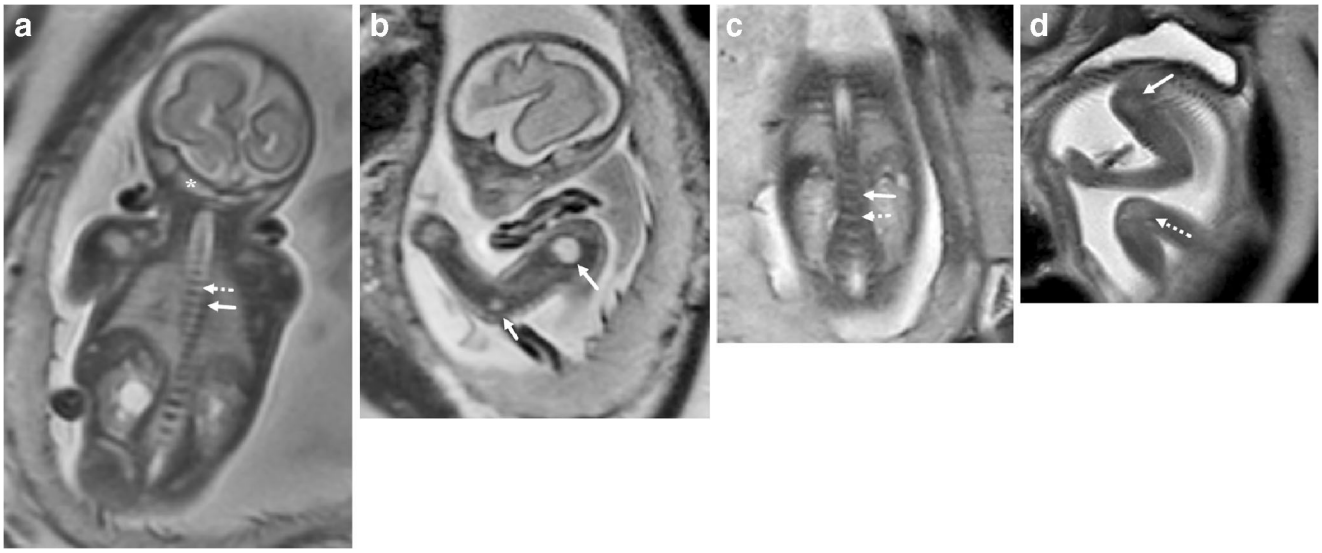

Fig. 3 Kniest dysplasia in a fetus at 26 weeks. **a** Coronal single-shot fast spin echo (SSFSE) T2-weighted image demonstrates enlarged T2 hyperintense disc (*dotted arrow*) with small dark intervening vertebrae (*solid arrow*). Note that the skull base is also hyperintense (*asterisk*). **b** Sagittal SSFSE T2-weighted image of the upper extremity demonstrates abnormally T2 hyperintense epiphyseal centers (*arrows*). For comparison, normal images are provided: **c** Normal spine at 24 weeks demonstrates slightly hyperintense intervening disc (*dotted arrow*) and normal size dark T2 vertebrae (*solid arrow*). **d** Normal fetus at 24 weeks with normal signal of the humeral (*solid arrow*) and femoral (*dotted arrow*) epiphyseal centers

and that the disease is uniformly lethal, we believe performing fetal MRI to rule thanatophoric dysplasia in or out is clinically impactful and a reason for pursuing fetal MRI in the prenatal workup of suspected skeletal dysplasia.

Another skeletal dysplasia for which we observed brain, and also spine, findings on fetal MRI is achondroplasia. Narrow craniocervical junction, deep transverse sulcus of the inferior temporal lobe surface, oversulcation of the temporal lobe and incomplete hippocampal rotation were highly sensitive and

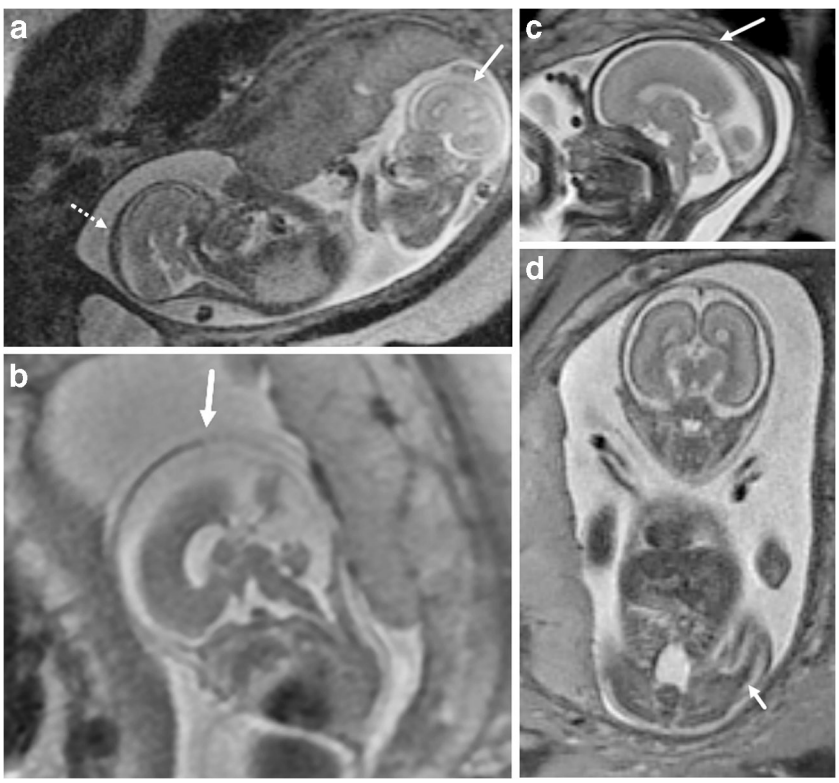

Fig. 4 Fetuses with osteogenesis imperfecta, Type II. **a** Twins at 21 weeks, one demonstrating abnormal calvarial ossification (*solid arrow*) and the other normal ossification (*dotted arrow*). **b** Sagittal T2-weighted image in a fetus at 24 weeks with poorly defined calvarium (*arrow*) due to lack of mineralization. **c** Normal fetus at 24 weeks with normal calvarial ossification (*arrow*) for comparison. **d** Coronal T2-weighted image of the lower extremity of a 22 weeks' gestation fetus with bowing of the distal extremity (*arrow*)

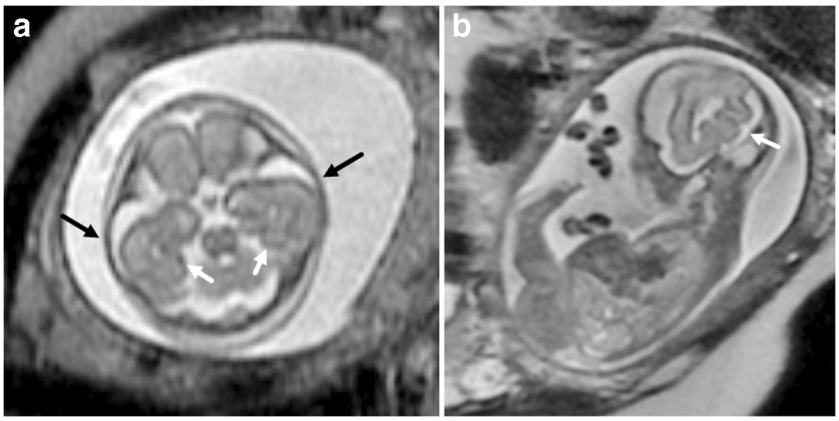

Fig. 5 Fetuses with thanatophoric dysplasia **a** Axial single-shot fast spin echo (SSFSE) T2-weighted image of the brain of a 21 weeks' gestation fetus demonstrates temporal lobe sulcation abnormality (*white arrows*) and abnormal calvarial contour (*black arrows*). **b** Sagittal SSFSE T2-weighted image of a 20 weeks' gestation fetus again demonstrates the temporal lobe sulcation abnormality (*arrow*). Notice the small chest and foreshortened lower extremity

specific findings, and the findings of prominent extra-axial fluid spaces, thoracolumbar kyphosis and small spinal canal were highly sensitive, but not specific, for achondroplasia. These brain and spine findings have been previously demonstrated by MRI in children with achondroplasia, and the finding of a narrowed craniocervical junction has been previously demonstrated in fetuses with achondroplasia by fetal MRI [17, 26, 27]. Thus, we believe fetal MRI is useful in supporting the prenatal diagnosis of achondroplasia.

Typical radiographic findings of osteogenesis imperfecta include osteopenia, fractures and micromelia [28]. One case report of a fetus with osteogenesis imperfecta Type II who underwent fetal MRI reported findings of fractures and pulmonary hypoplasia [29]. In our study, we found that the finding of limb bowing (a surrogate for fracture) on fetal MRI was present in all cases of osteogenesis imperfecta (Types II, III or IV). However, this finding was not specific for osteogenesis imperfecta and was also seen with intrinsic bone deformation in thanatophoric dysplasia and campomelic dysplasia. Another finding observed in cases of osteogenesis imperfecta (including Types II and III) was a poorly ossified calvarium, which we observed more frequently in Type II, the perinatal lethal type, than in Type III. Thus, the combination of two findings (limb bowing and poor ossification of the calvarium) provides good diagnostic ability to identify osteogenesis imperfecta.

For the remainder of specific skeletal dysplasia diagnosis, there were only one or two cases included. However, for some of these cases, there were findings on fetal MRI that aided in diagnosis, including the cartilage signal abnormality in Kniest dysplasia, which has been previously reported on fetal MRI for this same case [19], spine changes (vertebral bodies with abnormal morphology and mineralization) in achondrogenesis Type II, which have been reported in the literature by ultrasound and not with fetal MRI (to our knowledge) [30], and omphalocele in Boomerang dysplasia, for which there is a known association [31]. Jeune syndrome had no MRI findings to help confirm diagnosis. However, importantly, a normal brain was observed on fetal MRI in the cases of Jeune syndrome, Boomerang dysplasia, campomelic dysplasia, Kniest dysplasia and osteogenesis imperfecta, which may be in itself diagnostically useful.

Our study had several limitations. First, it included a small sample size, split across the different skeletal dysplasia diagnoses, which limited our ability to assess diagnostic performance. Second, our sample did not include a broad range of different diagnoses, so we cannot make conclusions regarding fetal MRI for other types of skeletal dysplasias. Third, this was a retrospective study, so our data were nonuniform. MRIs were obtained with different protocols and at varying gestational ages, and interpreting radiologists had varied clinical information available to them. Furthermore, genetic testing and outcome data were not obtained/available for all cases, including those without skeletal dyplasia, and, given the wide time range of the study, utilization and available genetic testing likely changed over the years. Finally, our retrospective review of images did not include blinding to disease diagnosis, which may have biased the interpretation. Similarly, at the time of clinical interpretation, radiologists had US reports and, in some cases, US images available. However, we believe that given the lack of published literature regarding fetal MRI series for skeletal dysplasia, our results are important and may be useful to providers caring for fetuses with skeletal dysplasia.

Conclusion

Fetal MRI is a good adjunctive diagnostic tool for skeletal dysplasia, especially in cases where prenatal US does not provide a specific diagnosis and prognosis is uncertain. In addition to the previously demonstrated utility for measuring fetal

lung volumes, which predict lethality, fetal MRI demonstrates findings of the brain in achondroplasia and thanatophoric dysplasia, of the spine in achondroplasia and achondrogenesis Type II, of the calvarium in osteogenesis imperfecta and thanatophoric dysplasia, of the cartilage in Kniest dysplasia, and other associated findings of rare skeletal dysplasia diagnoses. With the information that fetal MRI can provide, earlier genetic counseling and testing may be possible.

Compliance with ethical standards

Conflicts of interest None

References

1. Bonafe L, Cormier-Daire V, Hall C et al (2015) Nosology and classification of genetic skeletal disorders: 2015 revision. Am J Med Genet A 167A:2869–2892
2. Orioli IM, Castilla EE, Barbosa-Neto JG (1986) The birth prevalence rates for the skeletal dysplasias. J Med Genet 23:328–332
3. Dighe M, Fligner C, Cheng E et al (2008) Fetal skeletal dysplasia: an approach to diagnosis with illustrative cases. Radiographics 28: 1061–1077
4. Doray B, Favre R, Viville B et al (2000) Prenatal sonographic diagnosis of skeletal dysplasias. A report of 47 cases. Ann Genet 43:163–169
5. Gaffney G, Manning N, Boyd PA et al (1998) Prenatal sonographic diagnosis of skeletal dysplasias—a report of the diagnostic and prognostic accuracy in 35 cases. Prenat Diagn 18:357–362
6. Parilla BV, Leeth EA, Kambich MP et al (2003) Antenatal detection of skeletal dysplasias. J Ultrasound Med 22:255–258
7. Rahemtullah A, McGillivray B, Wilson RD (1997) Suspected skeletal dysplasias: femur length to abdominal circumference ratio can be used in ultrasonographic prediction of fetal outcome. Am J Obstet Gynecol 177:864–869
8. Ramus RM, Martin LB, Twickler DM (1998) Ultrasonographic prediction of fetal outcome in suspected skeletal dysplasias with use of the femur length-to-abdominal circumference ratio. Am J Obstet Gynecol 179:1348–1352
9. Teele RL (2006) A guide to the recognition of skeletal disorders in the fetus. Pediatr Radiol 36:473–484
10. Krakow D, Lachman RS, Rimoin DL (2009) Guidelines for the prenatal diagnosis of fetal skeletal dysplasias. Genet Med 11:127–133
11. Schramm T, Gloning KP, Minderer S et al (2009) Prenatal sonographic diagnosis of skeletal dysplasias. Ultrasound Obstet Gynecol 34:160–170
12. Victoria T, Zhu X, Lachman R et al (2018) What is new in prenatal skeletal dysplasias? AJR Am J Roentgenol 210:1022–1033
13. Miyazaki O, Nishimura G, Sago H et al (2012) Prenatal diagnosis of fetal skeletal dysplasia with 3D CT. Pediatr Radiol 42:842–852
14. Weaver KN, Johnson J, Kline-Fath B et al (2014) Predictive value of fetal lung volume in prenatally diagnosed skeletal dysplasia. Prenat Diagn 34:1326–1331
15. Fink AM, Hingston T, Sampson A et al (2010) Malformation of the fetal brain in thanatophoric dysplasia: US and MRI findings. Pediatr Radiol 40(Suppl 1):S134–S137
16. Suzumura H, Kohno T, Nishimura G et al (2002) Prenatal diagnosis of hypochondrogenesis using fetal MRI: a case report. Pediatr Radiol 32:373–375
17. Berceanu C, Gheonea IA, Vladareanu S et al (2017) Ultrasound and MRI comprehensive approach in prenatal diagnosis of fetal osteochondrodysplasias. Cases series. Med Ultrason 19:66–72
18. Miller E, Blaser S, Miller S et al (2008) Fetal MR imaging of atelosteogenesis type II (AO-II). Pediatr Radiol 38:1345–1349
19. Yazici Z, Kline-Fath BM, Laor T, Tinkle BT (2010) Fetal MR imaging of Kniest dysplasia. Pediatr Radiol 40:348–352
20. Teng SW, Guo WY, Sheu MH, Wang PH (2003) Initial experience using magnetic resonance imaging in prenatal diagnosis of osteogenesis imperfecta type II: a case report. Clin Imaging 27:55–58
21. Griffiths PD, Bradburn M, Campbell MJ et al (2017) Use of MRI in the diagnosis of fetal brain abnormalities in utero (MERIDIAN): a multicentre, prospective cohort study. Lancet 389:538–546
22. Kline-Fath B, Bahado-Singh R, Bulas D (2015) Fundamental and advanced fetal imaging: ultrasound and MRI. Wolters Kluwer, Philadelphia
23. Ngo AV, Thapa M, Otjen J, Kamps SE (2018) Skeletal dysplasias: radiologic approach with common and notable entities. Semin Musculoskelet Radiol 22:66–80
24. Blaas HG, Vogt C, Eik-Nes SH (2012) Abnormal gyration of the temporal lobe and megalencephaly are typical features of thanatophoric dysplasia and can be visualized prenatally by ultrasound. Ultrasound Obstet Gynecol 40:230–234
25. Stark Z, McGillivray G, Sampson A et al (2015) Apert syndrome: temporal lobe abnormalities on fetal brain imaging. Prenat Diagn 35:179–182
26. Manikkam SA, Chetcuti K, Howell KB et al (2018) Temporal lobe malformations in achondroplasia: expanding the brain imaging phenotype associated with FGFR3-related skeletal dysplasias. AJNR Am J Neuroradiol 39:380–384
27. Pugash D, Lehman AM, Langlois S (2014) Prenatal ultrasound and MRI findings of temporal and occipital lobe dysplasia in a twin with achondroplasia. Ultrasound Obstet Gynecol 44:365–368
28. Bulas DI, Stern HJ, Rosenbaum KN et al (1994) Variable prenatal appearance of osteogenesis imperfecta. J Ultrasound Med 13:419–427
29. Solopova A, Wisser J, Huisman TA (2008) Osteogenesis imperfecta type II: fetal magnetic resonance imaging findings. Fetal Diagn Ther 24:361–367
30. Kocakoc E, Kiris A (2002) Achondrogenesis type II with normally developed extremities: a case report. Prenat Diagn 22:594–597
31. Canki-Klain N, Stanescu V, Stanescu R et al (1992) Lethal short limb dwarfism with dysmorphic face, omphalocele and severe ossification defect: Piepkorn syndrome or severe "boomerang dysplasia"? Ann Genet 35:129–133